N^6-methyladenosine reader IGF2BP3 promotes endometrial cancer progression via modification of circ-EPB41L2 expression

LIPING LAI, XIAOXIAO FENG, YITING ZHENG and SHANRONG SHU

Department of Gynecology and Obstetrics, The First Affiliated Hospital of Jinan University, Guangzhou, Guangdong 510630, P.R. China

Received November 28, 2025; Accepted September 18, 2026

DOI: 10.3892/ol.2026.15937

Abstract. Endometrial cancer is one of the primary contributors to cancer-related mortality on a global scale. Insulin-like growth factor 2 mRNA binding protein 3 (IGF2BP3) is a reader protein of N^6-methyladenosine (m^6A) modifications and serves a key role in the carcinogenesis of numerous solid tumors. The present study explored the role and underlying mechanism of IGF2BP3 in endometrial cancer. Bioinformatics methods were applied to examine m^6A reader protein expression levels and their effect on survival. Reverse transcription-quantitative PCR and western blotting were used to determine IGF2BP3 expression in cancer and paracancerous tissues. After knockdown of IGF2BP3 expression, cell proliferation and migration were examined. Significantly expressed genes were identified through Kyoto Encyclopedia of Genes and Genomes and Gene Ontology analysis. Additionally, the cross-linking immunoprecipitation followed by high-throughput sequencing (CLIP-seq) database and methylated RNA immunoprecipitation (MeRIP) techniques were employed to ascertain the targets of IGF2BP3. The present study revealed that the expression levels of IGF2BP1, IGF2BP3, RNA binding motif protein 15 and YTH N^6-methyladenosine RNA binding protein C2 differed between normal and endometrial cancer tissue, based on The Cancer Genome Atlas analysis. Through examination of endometrial cancer tissues and Kaplan-Meier analysis, IGF2BP3 was determined to be a target for further research. Following knockdown of IGF2BP3 expression in HEC-1A cells using short hairpin RNA transfection, proliferation and migration were decreased compared with those in the control group. A transcriptome-wide RNA-sequencing assay indicated that circular RNA (circ) was abnormally expressed in endometrial carcinoma and was regulated by IGF2BP3. CLIP-seq database analysis and MeRIP suggested that circ-erythrocyte membrane protein band 4.1 like-2 (EPB41L2) was the target of IGF2BP3. IGF2BP3 was involved in the progression of endometrial cancer and served an oncogenic role by targeting circ-EPB41L2 in an m^6A-dependent manner.

Correspondence to: Professor Shanrong Shu, Department of Gynecology and Obstetrics, The First Affiliated Hospital of Jinan University, 613 Huangpu Road West, Guangzhou, Guangdong 510630, P.R. China
E-mail: butterfly1705@126.com

Key words: endometrial carcinoma, insulin-like growth factor 2 mRNA binding protein 3, circular RNA erythrocyte membrane protein band 4.1 like-2, N^6-methyladenosine

Introduction

Endometrial carcinoma comprises malignant tumors occurring in the female genital tract and is the third most common cause of gynecological cancer-related mortalities (1). The incidence and mortality rates have increased in recent years, with 66,200 new cases and 13,030 mortalities reported in 2023 in America (2). Despite advancements in diagnosis, targeted therapies and immunotherapies, the average 5-year survival rate of endometrial carcinoma is as low as 30%, especially for patients diagnosed in clinical phase III/IV, due to its rapid development and distant metastasis (3). Therefore, understanding the underlying molecular mechanism accounting for the carcinogenesis of endometrial carcinoma is essential for developing accurate targeted therapies.

Epigenetic modifications are involved in the carcinogenesis of numerous types of tumors, such as cervical (4) and hepatocellular (5) cancer. The N^6-methyladenosine (m^6A) modification of RNA is a reversible epigenetic modification, including for DNA methylation and histone modifications (6-8). m^6A-related proteins, referred to as 'writer', 'eraser' and 'reader' proteins, regulate pre-mRNA splicing, mRNA stability and the decay, localization, transport and translation of mRNA (9-12). The m^6A 'readers', such as YTH N^6-methyladenosine RNA binding protein C (YTHDC)1/2 and insulin-like growth factor 2 mRNA binding protein (IGF2BP)1/2/3, identify methylated RNA and participate in the translation and degradation of downstream proteins (13). IGF2BPs are considered to exert a key role in biological processes such as embryogenesis, cell migration, proliferation and invasion (14,15). IGF2BP3 recruits nudix hydrolase 21 to regulate SPTBN1 m^6A modifications, which drives ovarian cancer progression (16). IGF2BP3-methyltransferase like-14 complex regulates stearoyl-CoA desaturase mRNA m^6A modifications, resulting in cervical cancer cell proliferation, metastasis and increased lipid metabolism (17). IGF2BP3-mediated m^6A modification of the early growth response 1/PTEN axis regulates the malignant phenotypes of endometrial cancer stem cells (18).

IGF2BP3 enhances the mRNA stability of E2F transcription factor by interacting with long independently transcribed non-coding RNA 958 to promote endometrial carcinoma progression (19). Long non-coding RNA metastasis associated lung adenocarcinoma transcript 1 and urothelial cancer associated 1 can be used as biomarkers for the prognosis of patients with glioblastoma (20). Circular RNAs (circRNAs/circs) are dysregulated in nearly all types of cancer and drive tumorigenesis through tumor-suppressive functions (21). IGF2BP2-modified circ-chromodomain helicase DNA binding protein 7 promotes endometrial cancer progression by stabilizing platelet-derived growth factor receptor β and activating the Janus kinase/STAT signaling pathway (22).

CircEPB41L2 can bind PTBP1 and the E3 ubiquitin ligase TRIP12 to promote the ubiquitination and degradation of PTBP1, block the proliferation, invasion and metastasis of NSCLC (23), and act as a miRNA sponge involved in the tumorigenesis of colorectal cancer (24) and lung cancer (25).

However, the biological role of circEPB41L2 in gynecological diseases, and whether IGF2BP3 can regulate circEPB41L2 expression has not been reported. The present study explored IGF2BP3 expression in endometrial carcinoma and identified the underlying mechanism and signal pathway, which can be further explored for targeted treatment in endometrial carcinoma.

Materials and methods

Cell culture and clinical specimens. A total of 25 endometrial carcinoma and adjacent paracancerous tissues were collected from the same female patients with endometrial carcinoma who underwent tumor resection at The First Affiliated Hospital of Jinan University (Guangzhou, China) between August 2024 and December 2025. Adjacent normal tissues were collected at least 1 cm away from the tumor margin. Patients who had received chemotherapy, radiotherapy or hormonal therapy were excluded. The age of the patients ranged 42-65 years, and the mean age was 55.3 years. All patients provided written informed consent. Clinical stages were classified according to the International Federation of Gynecology and Obstetrics 2023 guidelines (26). The clinical parameters of the patients are summarized in Table I. The experimental procedures were approved by the Ethics Committee of The First Affiliated Hospital of Jinan University (Guangzhou, China; approval no. KY-2025-317).

The HEC-1A endometrial carcinoma cell line was obtained from American Type Culture Collection. HEC-1A cells were cultured at 37˚C with 5% CO_2 in DMEM (Gibco; Thermo Fisher Scientific, Inc.) supplemented 1% penicillin-streptomycin solution and 10% fetal calf serum (Gibco; Thermo Fisher Scientific, Inc.).

Functional annotation and pathway enrichment analysis. Gene set enrichment analysis software (version 4.3.2; https://www.gsea-msigdb.org/gsea/index.jsp) was used to perform Gene Ontology (GO) functional annotation and Kyoto Encyclopedia of Genes and Genomes (KEGG) pathway analyses. P<0.05 was considered to indicate a statistically significant difference. Volcano plots displayed the differentially expressed genes or circ RNA, and the top 20 genes were further analyzed. Differentially expressed genes were screened with the threshold of $|\log_2 FC|>1$ and false discovery rate (FDR)<0.05. Genes with $\log_2 FC>1$ and FDR<0.05 were defined as upregulated genes, while genes with $\log_2 FC<-1$ and FDR<0.05 were defined as downregulated genes.

Analysis of the prognostic and diagnostic performance of IGF2BP3. IGF2BP3 gene expression profiles and matched clinical follow-up data were retrieved from the Uterine Corpus Endometrial Carcinoma (UCEC) cohort of The Cancer Genome Atlas (TCGA) database (https://portal.gdc.cancer.gov) Patients were stratified into high- and low-IGF2BP3 groups according to the median expression level of IGF2BP3. Kaplan-Meier survival curves were plotted for overall survival (OS) and disease-free survival (DFS), and the log-rank test was used to compare survival differences between groups. Hazard ratios (HRs) with 95% confidence intervals were calculated. A receiver operating characteristic curve was constructed and the area under the curve was calculated to evaluate the diagnostic performance of IGF2BP3. All statistical analyses were performed in R software (version 4.3.1; https://www.R-project.org/).

Generation of cell lines with stable knockdown. Endogenous IGF2BP3 (NM_006547.3) was stably knocked down using lentiviral vectors containing short hairpin RNA (shRNA/sh) constructs: shIGF2BP3#1, 5'-CCTTGAAAGTAGCCTATAT-3'; shIGF2BP3#2, 5'-GGTGAAACTTGAAGCTCAT-3'; and shIGF2BP3#3, 5'-CCAGACACCTGATGAGAAT-3'. The sequence of the shRNA control was as follows: 5'-CCTAAGGTTAAGTCGCCCT-3'. Validated pLKO.1-based shRNA and scramble control plasmids were purchased from MilliporeSigma and used at 1 μg/μl. Lentivirus was packaged in 293T cells (MilliporeSigma) using a third-generation system. In brief, 3 μg of plasmids (transfer:psPAX2:pMD2.G-=4:3:1) were transfected into 70-80% confluent 293T cells per 6-well plate via Lipofectamine 3000 (Thermo Fisher Scientific, Inc.). Viral supernatants were collected at 48-72 h, sterile-filtered (0.45 μm) and stored at -80˚C. Target cells were transduced at an MOI of 2 for 24 h with 8 μg/ml polybrene. After medium renewal, antibiotic selection was performed at 48 h post-transduction to establish stable knockdown cell lines. All downstream experiments were conducted at 72 h after transduction.

Bioinformatic prediction of IGF2BP3-binding circRNAs. Potential circRNA targets of IGF2BP3 were predicted using ENCORI (starBase v2.0; https://starbase.sysu.edu.cn/) database, which curates and integrates published cross-linking immunoprecipitation followed by high-throughput sequencing (CLIP-seq) datasets for RNA-binding protein and RNA interaction analysis (27). Briefly, IGF2BP3 binding peaks we searched for and candidate circRNAs with statistically significant binding signals were retained. The default significance cut-off threshold of the ENCORI pipeline was applied, with FDR<0.05.

Cell Counting Kit-8 (CCK-8) assay. HEC-1A cells transfected with sh-negative control (sh-NC) or sh-IGF2BP3 were

Table I. Association of IGF2BP3 expression with clinicopathological features in 25 patients with endometrial carcinoma.

Variable	Total, n	IGF2BP3 (+), n=16	IGF2BP3 (-), n=9	P-value
Differentiation stage				0.0029
Well-moderate	18	15	3	
Poor	7	1	6	
FIGO stage				0.147
I-II	19	13	4	
III-IV	6	3	5	
Age, years				0.2203
<50	6	9	2	
≥50	19	7	7	
Pelvic lymph node metastasis				0.734
Yes	10	6	2	
No	15	10	7	

FIGO, International Federation of Gynecology and Obstetrics; IGF2BP3, insulin-like growth factor 2 mRNA binding protein 3.

seeded in 96-well plates (5,000 cells per well). After 24, 48, 72 and 96 h 0 μl CCK-8 solution (APExBIO Technology LLC) was added to each well. The cells were subsequently incubated for an additional 2 h at 37˚C. The absorbance was measured at a wavelength of 450 nm.

Transwell assay. A Transwell chamber (cat. no. 3422; Corning, Inc.) was used to detect cell migration. A total of $3x10^5$ cells suspended in serum-free medium were added to the upper chamber and 700 μl DMEM with 10% FBS was added to the lower chamber. For migration assays, uncoated upper chambers were applied. For invasion assays, upper chambers were pre-coated with Matrigel matrix (Corning, Inc.) and gelled at 37˚C. After incubation at 37˚C for 24 h, the upper chambers were rinsed with PBS and fixed in 100% methanol for 15 min at room temperature. Next, cells left on the surface of the chamber were carefully wiped off with cotton swabs. Crystal violet staining was performed for 10 min at room temperature, and then the lower chambers were rinsed again with PBS. Cells in three random fields were imaged under a bright-field microscope (magnification, x40) and the numbers of cells that had passed through the cell membrane were counted using ImageJ (version 1.54u8; National Institutes of Health).

Whole-transcriptome sequencing. Total RNA was isolated using TRIzol reagent (cat. no. 15596026; Thermo Fisher Scientific, Inc.). Ribosomal RNA depletion was performed using a Ribo-Zero rRNA Removal Kit (cat. no. MRZH11124; Illumina, Inc.). For quality verification, the RNA concentration and purity were determined using a Nanodrop 2000 spectrophotometer (Thermo Fisher Scientific, Inc.), and RNA integrity was assessed using an Agilent 2100 Bioanalyzer (Agilent Technologies, Inc.). Only samples with an optical density (OD)260/280 of 1.8-2.2, OD260/230 of 2.0-2.4 and RNA integrity number ≥7.0 were used for subsequent analysis.

Whole-transcriptome libraries were constructed using a TruSeq Stranded Total RNA Library Prep Kit (cat. no. 20020596; Illumina, Inc.). The final library concentration was accurately quantified with a Qubit 4.0 Fluorometer (Invitrogen; Thermo Fisher Scientific, Inc.), and libraries were normalized to a loading concentration of 1.5 nM. Sequencing was performed on the Illumina NovaSeq 6000 platform (Illumina, Inc.) with the paired-end 150-bp sequencing mode.

Raw sequencing reads were quality-trimmed and filtered using Trimmomatic v0.39 (www.usadellab.org/cms/page=trimmomatic). Clean reads were aligned to the human reference genome using HISAT2 v2.2.1 (https://daehwankimlab.github.io/hisat2/). Transcript expression levels (transcripts per million) were quantified using StringTie v2.2.1(https://ccb.jhu.edu/software/stringtie/). Differential expression analysis was conducted using DESeq2 v1.52.0 (R v4.6.1), with thresholds of $|\log_2 FC| \geq 1$ and adjusted $P<0.05$. All software was used with default parameters as documented in the official developer manuals.

RT-qPCR. Total RNA was extracted from cells or tissue using TRIzol Reagent (Invitrogen; Thermo Fisher Scientific, Inc.) in accordance with the manufacturer's protocol. The PrimeScript™ RT reagent kit (Takara Biotechnology Co., Ltd.) was used to reverse transcribe RNA into cDNA. The reaction program was set as 42˚C for 2 min (gDNA elimination), 37˚C for 15 min (reverse transcription) and 85˚C for 5 sec (heat inactivation). The cDNA was preserved at -20˚C. For qPCR, the reaction system was constructed according to the protocol of the SYBR Premix Ex Taq™ II kit (Takara Bio, Inc.). The expression levels of RNA were determined using the Bio-Rad CFX96 real-time PCR system (Bio-Rad Laboratories, Inc.). The human housekeeping gene GAPDH was used as the internal control. The sequences of the primers utilized in the present study were as follows: IGF2BP3 forward, 5'-CCGTATCCAAGCAGAAACCA-3' and reverse, 5'-AATCGACTTCTCAGCAGCCC-3'; GAPDH forward, 5'-AAGGCTGTGGGCAAGG-3' and reverse, 5'-TGGAGG AGTGGGTGTCG-3'; circ-EPB41L2 forward, 5'-ACCAAG GAAGTGCAGACCAA-3' and reverse, 5'-TCACTTCAGACA

CAGAGCCT-3'; circ-WDPCP forward, 5'-AACGATGAT GCTTGGCCTTG-3' and reverse, 5'-TCTGAGATGAGCTTC CCCAC-3'; and circ-PH20 forward, 5'-GAACCGACTTCT CCCCTTGT-3' and reverse, 5'-AGGCCTAGCATTACCCAC AA-3'. The thermocycling conditions were as follows: One cycle at 95˚C for 10 min, followed by 40 cycles of 95˚C for 15 sec and 60˚C for 60 sec. Melting curves were generated to confirm specific amplification. Relative gene expression was quantified by $2^{-\Delta\Delta Cq}$ method (28), normalized to GAPDH.

Western blot analysis. After PBS washing, cells were lysed in RIPA buffer (cat. no. R0010; Beijing Solarbio Science & Technology Co., Ltd.) supplemented with 1% PMSF (cat. no. P0100; Beijing Solarbio Science & Technology Co., Ltd.) on ice for 30 min. Lysates were centrifuged at 12,000 x g for 15 min at 4˚C and protein concentrations were quantified using a BCA assay kit (cat. no. MA0082; Dalian Meilun Biotechnology Co., Ltd.). Proteins (30 mg/lane) were separated by SDS-PAGE (cat. no. P0015L; Beyotime Biotechnology) and transferred to PVDF membranes (Roche Diagnostics). Membranes were blocked with quick block buffer (cat. no. P0023B; Beyotime Biotechnology) at room temperature for 30 min and incubated with primary antibodies IGF2BP1 (1:1,500; cat. no. ab184305; Abcam) IGF2BP3 (1:2,000; cat. no. ab225697; Abcam) and GAPDH (1:1,000; cat. no. MA5-15738; Thermo Fisher Scientific, Inc.) overnight at 4˚C. After incubation with horseradish peroxidase-conjugated secondary antibody IgG (H+L) (1:1,000; cat. no. A0352; Beyotime Biotechnology) for 1 h at room temperature, protein bands were visualized using ECL reagent (cat. no. MA0186; Dalian Meilun Biotechnology Co., Ltd.).

Methylated RNA immunoprecipitation (MeRIP). MeRIP analysis was performed according to MeRIP m^{6}A kit (cat. no. C11051-1; Guangzhou RiboBio Co., Ltd). Total RNA was extracted and chemically fragmented at 70˚C for 5 min to produce 100-200 nucleotide RNA fragments. For each IP reaction, 100 μg fragmented RNA was incubated with the kit-supplied anti-m^{6}A antibody and Protein A/G magnetic beads at 4˚C overnight; IgG from the kit served as the negative control. The bead-RNA-antibody complexes were washed three times with pre-cooled 1X IP buffer. Immunoprecipitated RNA was eluted, purified and subjected to RT-qPCR to evaluate m^{6}A enrichment.

Statistical analysis. All experiments were performed in triplicate with consistent and reproducible results. Statistical analysis was carried out using SPSS 16.0 software (SPSS, Inc.), and data are presented as the mean ± SD. Comparisons between two groups were performed using t-tests. Matched samples were analyzed using a paired-samples t-test. For independent samples, the homogeneity of variance test was performed first to select the appropriate test. If the variance was homogeneous ($P>0.05$), independent-samples t-test was used for group comparison. One-way ANOVA was performed to analyze differences among multiple groups, with Tukey's test adopted for post hoc pairwise comparisons. The associations between IGF2BP3 expression and clinicopathological features were analyzed using Fisher's exact test. $P<0.05$ was considered to indicate a statistically significant difference.

Results

m^{6}A reader proteins are involved in endometrial carcinoma. First, the expression levels of the m^{6}A methylation-related reader proteins in 35 normal and 546 endometrial carcinoma tissues from TCGA database were compared and analyzed (Fig. 1A). IGF2BP1, IGF2BP3 and RNA binding motif protein 15 (RBM15) were revealed to be upregulated, while YTHDC2 was downregulated in endometrial carcinoma. Upregulated expression of IGF2BP1, IGF2BP3 and RBM15, but downregulated expression of YTHDC2 was associated with poorer survival (Fig. 1B). To further verify the expression of the aforementioned genes, qPCR was performed for 5 pairs of endometrial carcinoma tissues and corresponding paracancerous tissues. The results indicated that only IGF2BP1 and IGF2BP3 were expressed at significantly higher levels in endometrial cancer tissues (Fig. 1C). Subsequently, 25 clinical samples were used to further detect the expression levels of IGF2BP1 and IGF2BP3 by RT-qPCR and western blotting. AlthoughIGF2BP3 and IGF2BP1 expression was significantly upregulated in endometrial carcinoma tissues compared with paracancerous tissues, only the mRNA and protein expression of IGF2BP3 was consistently increased (Fig. 1D and E). Therefore, IGF2BP3 was selected as the target gene to perform further research.

Association of IGF2BP3 with unfavorable prognosis in endometrial carcinoma. To further explore the association between IGF2BP3 expression and patient prognosis, the overall survival (OS) and The DFS and OS rates of patients with endometrial carcinoma were evaluated via Kaplan-Meier survival analysis. Patients with high IGF2BP3 expression exhibited significantly shorter OS and DFS times (Fig. 2A and B). Furthermore, the potential diagnostic value of IGF2BP3 expression in endometrial carcinoma was evaluated using a receiver operating characteristic curve. As shown in Fig. 2C, the area under the curve for IGF2BP3 was 0.76 with a sensitivity of 80% and a specificity of 65%.

IGF2BP3 facilitates the proliferation and migration of endometrial carcinoma cells in vitro. To determine the biological role of IGF2BP3 *in vitro*, HEC-1A endometrial carcinoma cells were transfected with sh-IGF2BP3 or sh-NC. The knockdown efficiency of IGF2BP3 was verified by RT-qPCR (Fig. 3A). sh-IGF2BP3-1 and sh-IGF2BP3-3 significantly reduced the mRNA level of IGF2BP3, while sh-IGF2BP3-2 showed no notable knockdown effect Flow cytometry was used to evaluate lentiviral infection efficiency by detecting EGFP fluorescence (Fig. 3B). The EGFP-positive rates of all three groups exceeded 93%, indicating satisfactory lentivirus transduction for subsequent functional experiments. Western blot analysis demonstrated that IGF2BP3 protein expression was significantly decreased after transfection with sh-IGF2BP3-1. (Fig. 3C). Therefore, sh-IGF2BP3-1 and sh-IGF2BP3-3 were used to detect functional changes in HEC-1A cells. The results indicated that downregulation of IGF2BP3 significantly decreased cell viability (Fig. 3D). Transwell migration and invasion assays demonstrated that knockdown of IGF2BP3 markedly suppressed cell migration and invasion compared with the sh-NC group (Fig. 3E).

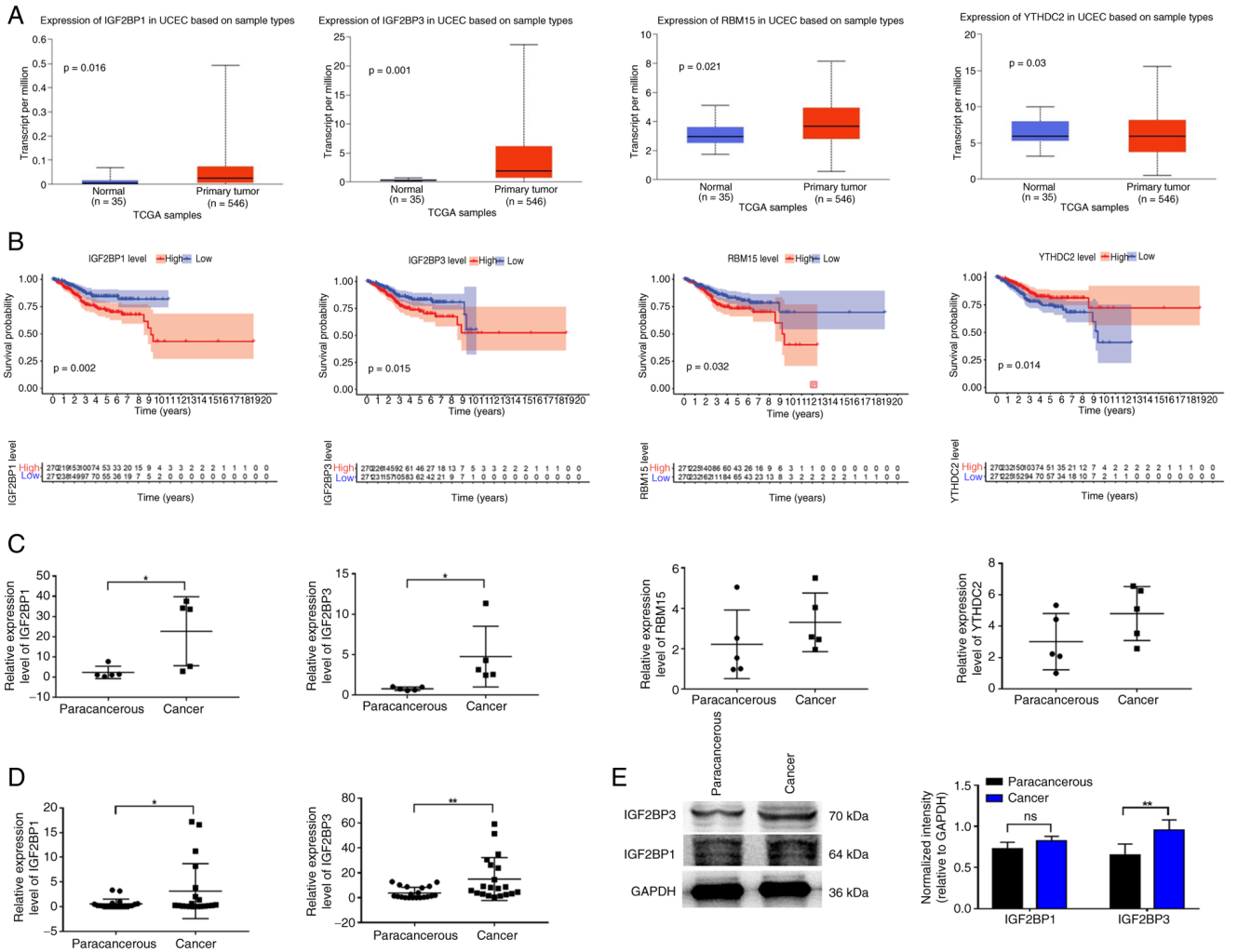


Figure 1. N^6-methyladenosine reader protein expression in endometrial carcinoma. (A) IGF2BP1, IGF2BP3, RBM15 and YTHDC2 expression in normal and tumor tissues from TCGA. (B) Kaplan-Meier analysis of patients with high/low expression of IGF2BP1, IGF2BP3, RBM15 and YTHDC2. (C) IGF2BP1, IGF2BP3, RBM15 and YTHDC2 expression was upregulated in cancer compared with paracancerous tissues from the GEO database. (D) IGF2BP1 and IGF2BP3 mRNA expression in cancer and paracancerous tissues. (E) IGF2BP1 and IGF2BP3 protein expression in cancer and paracancerous tissues. An unpaired-samples t-test was used in the analysis of normal and tumor tissues from TCGA in (A), while a paired t-test was used to analyze the data in (C-E). *P<0.05, **P<0.01. ns, not significant; IGF2BP, insulin-like growth factor 2 mRNA binding protein; RBM15, RNA binding motif protein 15; YTHDC2, YTH N^6-methyladenosine RNA binding protein C2; TCGA, The Cancer Genome Atlas; UCEC, uterine corpus endometrial carcinoma.

Identification of the circRNA expression profile in endometrial carcinoma. CircRNAs are considered to serve a key role in the clinical diagnosis, treatment and prognosis evaluation of tumors due to their high stability and tissue specificity (29). RNA-sequencing analysis of endometrial carcinoma tissue and paracancerous tissue was performed. A total of 168 circRNAs were upregulated and 273 circRNAs were downregulated in tumor tissue (Fig. 4A). KEGG and GO analysis indicated that the significantly altered genes were involved in 'regulation of transcription' and 'cellular response to DNA damage stimulus' and associated with the 'TGF-β signaling pathway' and the 'Wnt signaling pathway' (Fig. 4B). Furthermore, the downregulation of IGF2BP3 resulted in dysregulated gene expression, including upregulation of 178 genes and downregulation of 232 genes, in transfected endometrial carcinoma cells (Fig. 4C). The significantly altered terms and pathways included 'cellular heat acclimation', the 'transmembrane receptor protein tyrosine kinase signaling pathway', the 'Wnt signaling pathway' and 'MAPK, PI3K-Akt pathway' (Fig. 4D). These results suggested that circRNAs were abnormally expressed in endometrial carcinoma and may be regulated by IGF2BP3.

IGF2BP3 regulates circ-EPB41L2 in an m^{6}A-dependent manner. To determine the specific targeted circRNA which corresponded to IGF2BP3, screening of candidate circRNAs regulated by IGF2BP3 was performed using the CLIP-seq database according to the following criteria: i) The trend of circRNA expression was consistent with that of IGF2BP3, namely, the expression of circRNA in endometrial cancer was dysregulated; ii) the expression of circRNA was down-regulated after interference with IGF2BP3 expression; and iii) the circRNA simultaneously had m^{6}A and IGF2BP3 binding sites. Based on the aforementioned criteria, three circRNAs (circ-EPB41L2, circ-WD repeat containing planar cell polarity effector and circ-PH20) were predicted to interact with IGF2BP3 (Fig. 5A). Pairs supported by ≥2 independent CLIP-seq experiments (ClipExpNum ≥2) were considered for subsequent analysis.

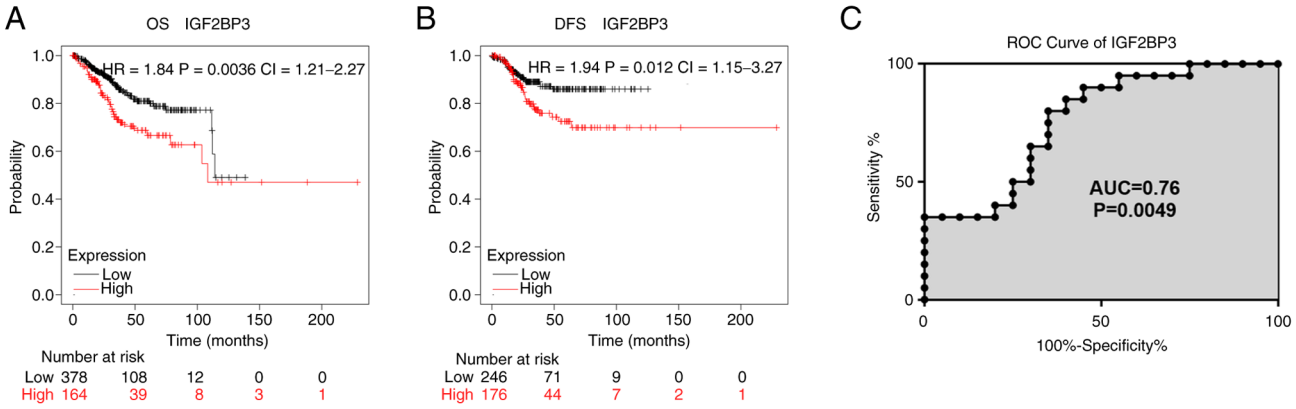


Figure 2. Survival analysis of patients with endometrial cancer using Gene Expression Profiling Interactive Analysis. (A) OS rate assessed by Kaplan-Meier analysis. (B) RFS assessed by Kaplan-Meier analysis. (C) Evaluation of the potential diagnostic value of IGF2BP3 using an ROC curve. OS, overall survival; IGF2BP3, insulin-like growth factor 2 mRNA binding protein 3; ROC, receiver operating characteristic; AUC, area under the curve; RFS, recurrence-free survival; HR, hazard ratio.

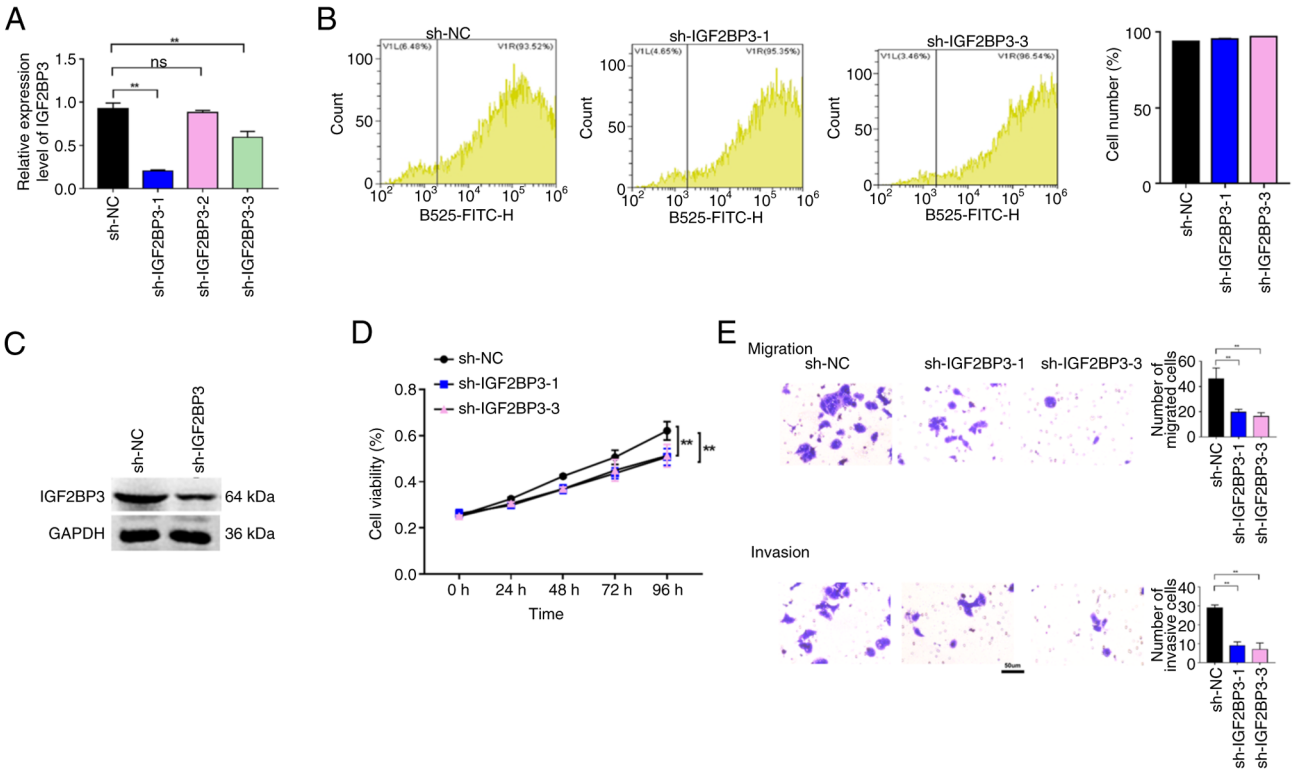


Figure 3. IGF2BP3 regulates the proliferation and migration of endometrial cancer cells. (A) IGF2BP3 expression in sh-NC and sh-IGF2BP3 groups was determined by reverse transcription-quantitative PCR. (B) Transfection efficacy was determined by flow cytometry. EGFP excited by 488 nm laser emits green fluorescence at 509 nm, detected via the FITC (B525) channel. Successfully transfected cells are fluorescence-positive (V1R) and non-transfected cells are negative (V1L). Transfection efficiency is the percentage of positive cells. (C) IGF2BP3 expression in the sh-NC and sh-IGF2BP3 groups was examined by western blotting. (D) Proliferation of cells in the sh-NC and sh-IGF2BP3 groups was determined using an CCK-8assay. (E) Migration of cells in the sh-NC and sh-IGF2BP3 groups was determined by Transwell assay. One-way ANOVA followed by Tukey's multiple comparison test t were used to analyze data. **P<0.01. IGF2BP3, insulin-like growth factor 2 mRNA binding protein 3; sh, short hairpin RNA; NC, negative control; ns, not significant. P1, population 1; V1L, gate V1 left; V1R, gate V1 right; B525, blue laser; FITC, fluorescein isothiocyanate. EGFP enhanced green fluorescent protein.

Among them, circ-EPB41L2 was prioritized for further investigation as it exhibited the most consistent IGF2BP3 binding in CLIP-seq datasets and the most marked upregulation in endometrial cancer tissues relative to paired paracancerous control tissues (Fig. 5B). Functional validation in HEC-1-A cells suggested that only circ-EPB41L2 expression was significantly reduced following IGF2BP3 knockdown (Fig. 5C), whereas the expression of the other two candidates was not statistically significantly altered.

An m^{6}A RIP (Fig. 5D) assay verified that circ-EPB41L2 can be dynamically modulated by m^{6}A modification supporting a potential regulatory axis involving m^{6}A modification and IGF2BP3 binding. Collectively, these findings identified circ-EPB41L2 as a key target for future mechanistic studies.

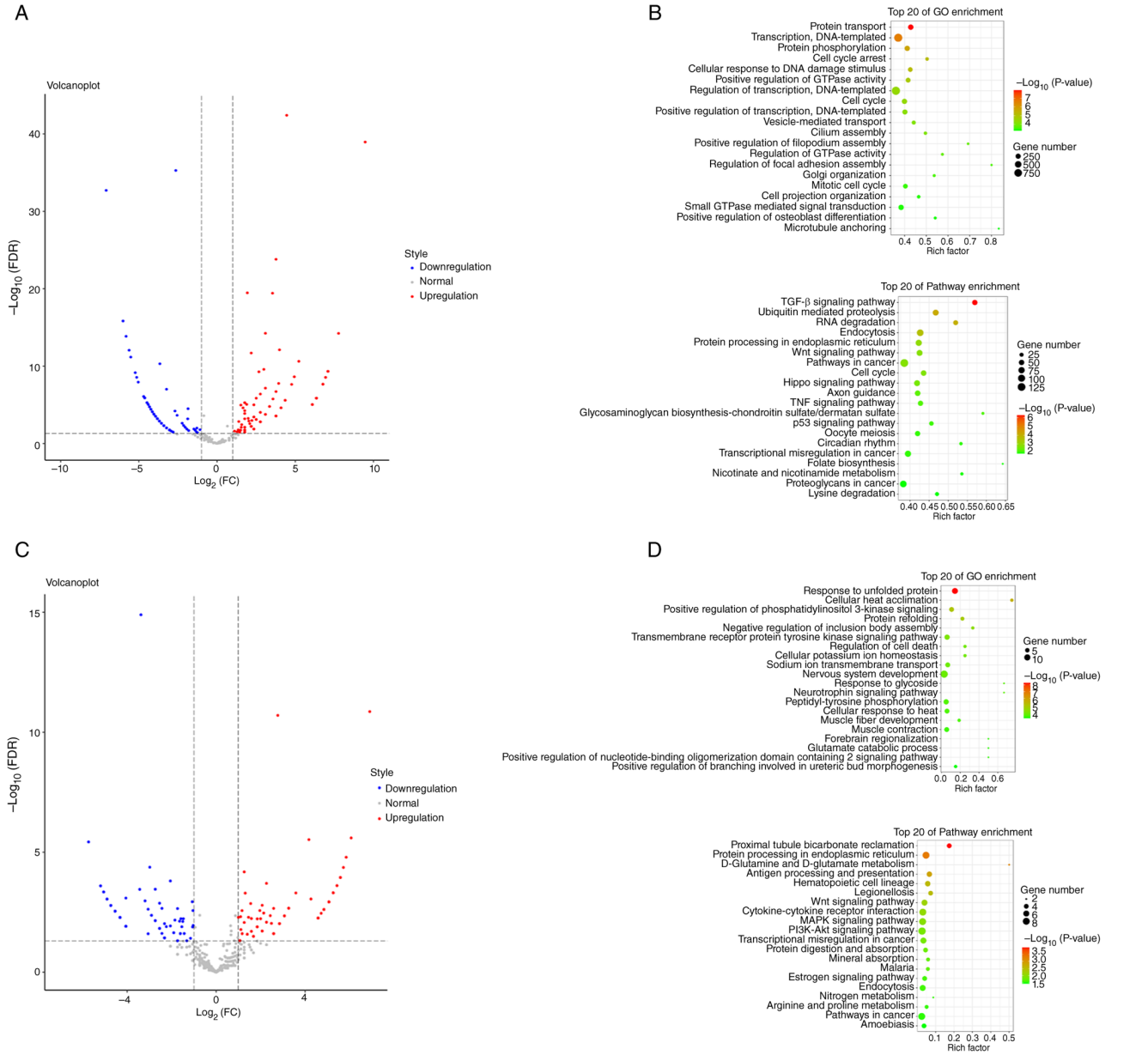


Figure 4. Bioinformatics analysis of the potential targets of IGF2BP3. (A) Volcano plot of differentially expressed genes in endometrial carcinoma tissue and para-cancer. Gene expression changes (Log_2FC) and significance ($log_{10}FDR$) are plotted. Genes beyond both fold-change and FDR thresholds are defined as significantly upregulated (red) or downregulated (blue); others (gray) show no significant difference. (B) KEGG and GO analysis of enriched terms and signaling pathways. (C) Volcano plot showing differentially expressed genes after downregulation of IGF2BP3. Gene expression changes (Log_2FC) and significance ($log_{10}FDR$) are plotted. Genes beyond both fold-change and FDR thresholds are defined as significantly upregulated (red) or downregulated (blue); others (gray) show no significant difference. (D) KEGG analysis of genes involved in the signal pathway after downregulation of IGF2BP3 (GF2BP3, insulin-like growth factor 2 mRNA binding protein 3; KEGG; Kyoto Encyclopedia of Genes and Genomes; GO, Gene Ontology; FDR, false discovery rate; RNA-seq, RNA-sequencing; FC, fold change.

Discussion

The reversible m^{6}A modification is considered to be the most abundant RNA modification, which serves a key role in regulating RNA splicing, stability and translation via writer, eraser and reader proteins (30). Inhibition of m^{6}A read protein YTHDF2 triggers proteotoxic cell death, which affects breast cancer progression (31). YTHDF1 associated with high-altitude hypoxia adaptation, modulates NSCLC progression and cisplatin sensitivity by regulating the translation of cell cycle genes and the Keap1/Nrf2/AKR1C1 axis (32). RNA-binding proteins have a variety of functions, of which the post-transcriptional regulation of gene expression is a key factor involved in carcinogenesis and therapeutic responses (33). Increased IGF2BP3 expression typically implies the malignant transformation of tissues (34). IGF2BP3 stabilizes PDPN mRNA to facilitate invadopodia formation and extracellular matrix degradation, promoting tumorigenesis and invasion in oral squamous cell carcinoma (35), the role of IGF2BP3 in endometrial carcinoma has rarely been explored.

In the present study, the expression levels of major m^{6}A methylation-related 'reader' proteins were compared and analyzed using TCGA, which suggested that IGF2BP1, IGF2BP3 and RBM15 were upregulated in endometrial

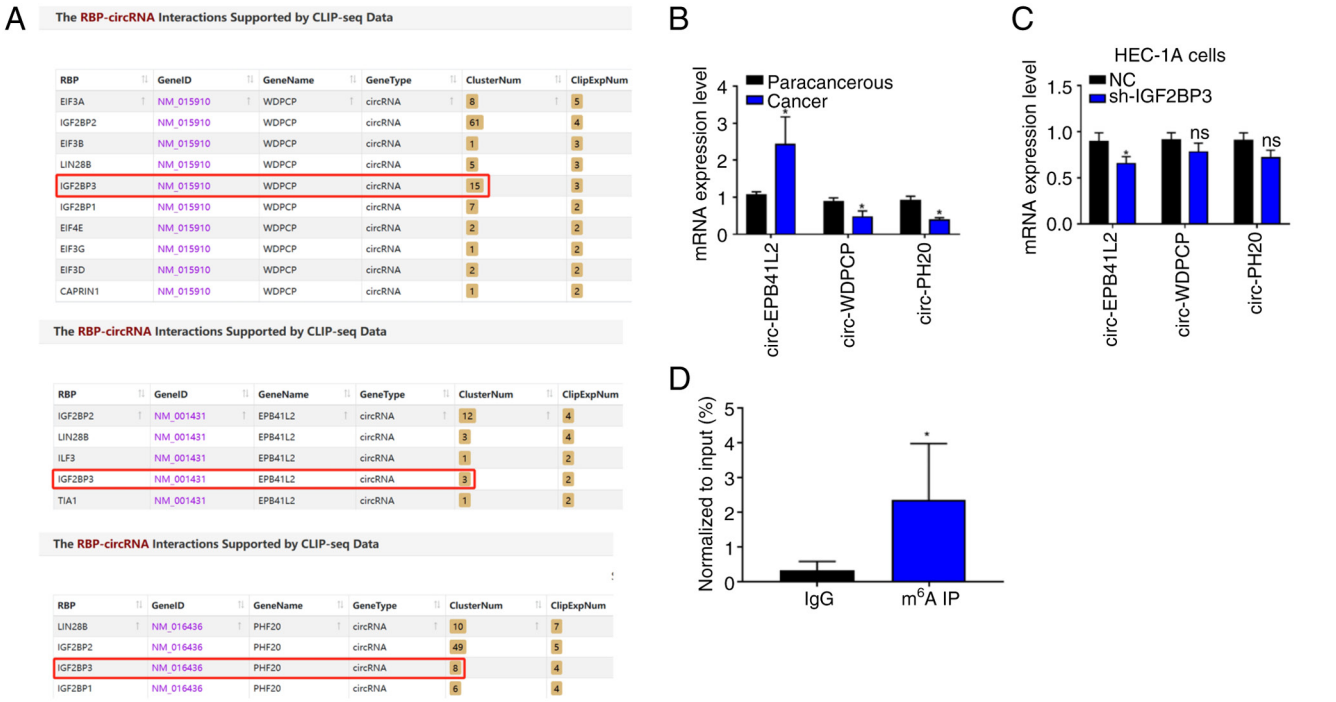


Figure 5. CLIP-seq database analysis and MeRIP determining the targets of IGF2BP3. (A) CLIP-seq database analysis was used to detect potential targets of IGF2BP3. (B) mRNA expression levels of the three potential circRNAs in cancer and paracancerous tissues. (C) mRNA expression levels of the three potential circRNA after downregulation of IGF2BP3 in HEC-1A cells. (D) MeRIP was used to determine whether IGF2BP3 modulates circ-EPB41L2 in an m^{6}A-dependent manner. Independent-samples t-tests were used to analyze the data in (C and D), whereas a paired-samples t-test was used to analyze the data in (B). *P<0.05. ns, not significant; NC, negative control; sh, short hairpin RNA; IGF2BP3, insulin-like growth factor 2 mRNA binding protein 3; MeRIP, methylated RNA immunoprecipitation; CLIP-seq, cross-linking immunoprecipitation followed by high-throughput sequencing; RBP, RNA binding protein; circRNA/circ, circular RNA; EPB41L2, erythrocyte membrane protein band 4.1 like-2; WDPCP, WD repeat containing planar cell polarity effector; PH20, PHD finger protein 20; IP, immunoprecipitation; m^{6}A, N^6-methyladenosine.

carcinoma. High expression levels of the upregulated proteins were associated with worse prognosis. Subsequently, the expression levels of the IGF2BP1 and IGF2BP3 were analyzed by RT-qPCR and western blotting. Lastly, IGF2BP3 was revealed to be the only gene that exhibited consistent expression changes at the mRNA and protein level and was related to the prognosis of patients. Although multivariate survival analysis was not performed to analyze the association between IGF2BP3 expression and clinicopathological parameters, IGF2BP3 was still selected as the target gene to perform further research.

IGF2BP3 is associated with the carcinogenesis and progression of numerous types of cancer. Chen *et al* (36) examined TCGA data and revealed that IGF2BP3 was predominantly upregulated across 18 different types of tumors. Consistent with this study, the present study revealed that IGF2BP3 was upregulated in patients with endometrial carcinoma. IGF2BP3-stabilized SIX homeobox 4 promotes the proliferation, migration, invasion and tube formation of ovarian cancer cells (37). IGF2BP3 interacts with MYCN and facilitates neuroblastoma cell proliferation (38). IGF2BP3, as a reader protein, prevents high mobility group box 1 mRNA decay in bladder cancer (39). In the present study, knockdown of IGF2BP3 expression inhibited cell proliferation and invasion *in vitro*. These results implied the role of IGF2BP3 in endometrial carcinoma development. Therefore, the mechanism of IGF2BP3 in endometrial carcinoma should be further explored.

circRNAs are involved in proliferation, metastasis, apoptosis, metabolism and drug resistance in urological cancer (40). circRNAs can not only combine with microRNAs to compete with endogenous RNA in colon cancer but also bind to certain proteins (41). circ-nuclear factor of activated T cells 3 promotes the proliferation of gastric cancer cells by binding to IGF2BP3 and restricting its ubiquitination to enhance cyclin D1 mRNA stability (42). circ-EPB41L2 serves as a potential diagnostic and prognostic biomarker in lung adenocarcinoma (43). However, how IGF2BP3 influences the expression of circ-EPB41L2 has not been explored. In the present study, a CLIP-seq database was used to predict genes that IGF2BP3 may bind to. circ-EPB41L2 expression was revealed to be positively associated with IGF2BP3 expression. Although IGF2BP3-RIP-qPCR, RNA pull-down assays, m^{6}A site mutation experiments, actinomycin D stability assays and reciprocal rescue experiments were not performed to demonstrate the direct association between IGF2BP3 and circ-EPB41L2, MeRIP demonstrated that IGF2BP3 effectively bound to circ-EPB41L2. In the future, Sanger sequencing and subcellular localization analysis should be performed to further confirm IGF2BP3 regulation of circ-EPB41L2 in an m^{6}A-dependent manner. Furthermore, it should be explored whether circ-EPB41L2 regulates ferroptosis in cancer progression, similar to long non-coding RNAs (44).

The present study demonstrated that IGF2BP3 was a tumorigenic RNA-binding protein that may mediate the stabilization of circ-EPB41L2. However, the detailed mechanisms of

IGF2BP3 and circ-EPB41L2 regulators need to be investigated further in the future.

The present study has several limitations. First, the patient sample size needs to be expanded. Second, m^6A methylation site prediction and functional verification should be performed at multiple levels to confirm the IGF2BP3-dependent epigenetic regulatory mechanism of circ-EPB41L2. Finally, additional cell and animal studies should be performed to further clarify the roles of IGF2BP3 and circ-EPB41L2 in endometrial carcinoma.

In summary, the present study provided *in vitro* evidence demonstrating that IGF2BP3 was a reader protein that could modify circ-EPB41L2, contributing to the tumorigenesis of endometrial cancer. IGF2BP3 may therefore be used as a target for the therapy of endometrial carcinoma.

Acknowledgements

Not applicable.

Funding

The present study was supported by the Science and Technology Projects in Guangzhou (grant no. 202102010134).

Availability of data and materials

The high-throughput sequencing data generated in the present study may be found in the Gene Expression Omnibus database under accession number GSE333959 or at the following URL: (www.ncbi.nlm.nih.gov/geo/query/acc.cgi?acc=GSE333959). The other data generated in the present study may be requested from the corresponding author.

Authors' contributions

LL participated in performing the experimental work and drafted the manuscript. XF performed the statistical analyses, prepared the figures and critically read and corrected the manuscript. YZ collected the specimens and performed the experimental work. SS participated in conceiving the study and received the financial support. All authors read and approved the final version of the manuscript. LL, XF, YZ and SS confirm the authenticity of all the raw data.

Ethics approval and consent to participate

Ethics approval was obtained from the Ethics Committee of The First Affiliated Hospital of Jinan University (Guangzhou, China; approval no. KY-2025-317). The procedures used in the present study adhere to the tenets of the Declaration of Helsinki. Written informed consent was obtained from all participants.

Patient consent for publication

Not applicable.

Competing interests

The authors declare that they have no competing interests.

References

1. Liang B, Tan J, Li J, Wang X, Li G, Li H, Li T and Gao H: Epidemiology, molecular typing, microbiome-immune interactions and treatment strategies of endometrial cancer: A review. Front Immunol 16: 1595638, 2025.
2. Siegel RL, Miller KD, Wagle NS and Jemal A: Cancer statistics, 2023. CA Cancer J Clin 73: 17-48, 2023.
3. Dane C and Bakir S: The effect of myometrial invasion on prognostic factors and survival analysis in endometrial carcinoma. Afr Health Sci 19: 3235-3241, 2019.
4. Liu H, Ma H, Li Y and Zhao H: Advances in epigenetic modifications and cervical cancer research. Biochim Biophys Acta Rev Cancer 1878: 188894, 2023.
5. Nagaraju GP, Dariya B, Kasa P, Peela S and El-Rayes BF: Epigenetics in hepatocellular carcinoma. Semin Cancer Biol 86: 622-632, 2022.
6. Koch A, Joosten SC, Feng Z, de Ruijter TC, Draht MX, Melotte V, Smits KM, Veeck J, Herman JG, Van Neste L, *et al*: Analysis of DNA methylation in cancer: Location revisited. Nat Rev Clin Oncol 15: 459-466, 2018.
7. Kraiczy J, Nayak KM, Howell KJ, Ross A, Forbester J, Salvestrini C, Mustata R, Perkins S, Andersson-Rolf A, Leenen E, *et al*: DNA methylation defines regional identity of human intestinal epithelial organoids and undergoes dynamic changes during development. Gut 68: 49-61, 2019.
8. Roundtree IA, Evans ME, Pan T and He C: Dynamic RNA modifications in gene expression regulation. Cell 169: 1187-1200, 2017.
9. Wang X, Zhao BS, Roundtree IA, Lu Z, Han D, Ma H, Weng X, Chen K, Shi H and He C: N(6)-methyladenosine modulates messenger RNA translation efficiency. Cell 161: 1388-1399, 2015.
10. Lin S, Choe J, Du P, Triboulet R and Gregory RI: The m(6)A methyltransferase METTL3 promotes translation in human cancer cells. Mol Cell 62: 335-345, 2016.
11. He L, Li H, Wu A, Peng Y, Shu G and Yin G: Functions of N6-methyladenosine and its role in cancer. Mol Cancer 18: 176, 2019.
12. Huang H, Weng H and Chen J: The biogenesis and precise control of RNA m(6)A methylation. Trends Genet 36: 44-52, 2020.
13. Jiang X, Liu B, Nie Z, Duan L, Xiong Q, Jin Z, Yang C and Chen Y: The role of m6A modification in the biological functions and diseases. Signal Transduct Target Ther 6: 74, 2021.
14. Bell JL, Wachter K, Muhleck B, Pazaitis N, Kohn M, Lederer M and Huttelmaier S: Insulin-like growth factor 2 mRNA-binding proteins (IGF2BPs): Post-transcriptional drivers of cancer progression? Cell Mol Life Sci 70: 2657-2675, 2013.
15. Degrauwe N, Suva ML, Janiszewska M, Riggi N and Stamenkovic I: IMPs: An RNA-binding protein family that provides a link between stem cell maintenance in normal development and cancer. Genes Dev 30: 2459-2474, 2016.
16. Luo X, Xie L, Ma X, Chen N, Xu J, Jiang X, Liu X, Yang Y, LiuT, Yi P and Xu J: IGF2BP3 recruits NUDT21 to regulate SPTBN1 alternative polyadenylation and drive ovarian cancer progression. Commun Biol 8: 680, 2025.
17. Han C, Hu C, Liu T, Sun Y, Hu F, He Y, Zhang J, Chen J, Ding J, Fan J, *et al*: IGF2BP3 enhances lipid metabolism in cervical cancer by upregulating the expression of SCD. Cell Death Dis 15: 138, 2024.
18. Wang B, Wang Y, Wang W, Wang Z, Zhang Y, Pan X, Wen X, Leng H, Guo J and Ma XX: WTAP/IGF2BP3 mediated m6A modification of the EGR1/PTEN axis regulates the malignant phenotypes of endometrial cancer stem cells. J Exp Clin Cancer Res 43: 204, 2024.
19. Wang C, Kong F, Ma J, Miao J, Su P, Yang H, Li Q and Ma X: IGF2BP3 enhances the mRNA stability of E2F3 by interacting with LINC00958 to promote endometrial carcinoma progression. Cell Death Discov 8: 279, 2022.
20. Hooshmandi S, Jangholi E, Heidarian A, Dehghani M, Ghassemi A, Heidary A, Rezvanimehr A, Sadeghi E, Ghodsi SM, Hoseinian M, *et al*: The role ofMALAT1 andUCA1 long noncodingRNAs on the prognosis of patients with glioblastoma: A systematic review and meta-analysis. Precis Med Sci 14: 66-74, 2025.
21. Conn VM, Chinnaiyan AM and Conn SJ: Circular RNA in cancer. Nat Rev Cancer 24: 597-613, 2024.
22. Shi R, Zhao R, Shen Y, Wei S, Zhang T, Zhang J, Shu W, Cheng S, Teng H and Wang H: IGF2BP2-modified circular RNA circCHD7 promotes endometrial cancer progression via stabilizing PDGFRB and activating JAK/STAT signaling pathway. Cancer Gene Ther 31: 1221-1236, 2024.

23. Wang Y, Wang Y, Wu C, Ji Y, Hou P, Wu X, Li Z, Li M, Chu S, Ning Q, *et al*: circEPB41L2 blocks the progression and metastasis in non-small cell lung cancer by promoting TRIP12-triggered PTBP1 ubiquitylation. Cell Death Discov 10: 72, 2024.
24. Jiang Z, Hou Z, Li L, Liu W, Yu Z and Chen S: Exosomal circEPB41L2 serves as a sponge for miR-21-5p and miR-942-5p to suppress colorectal cancer progression by regulating the PTEN/AKT signalling pathway. Eur J Clin Invest 51: e13581, 2021.
25. Zhang SJ, Ma J, Wu JC, Hao ZZ, Zhang YN and Zhang YJ: CircRNA EPB41L2 inhibits tumorigenicity of lung adenocarcinoma through regulating CDH4 by miR-211-5p. Eur Rev Med Pharmacol Sci 25: 3150, 2021.
26. Gaffney D, Suneja G, Weil C and Creutzberg C: International federation of gynecology and obstetrics endometrial 2023 is better for radiation oncology patients. Pract Radiat Oncol 14: 574-581, 2024.
27. Li JH, Liu S, Zhou H, Qu LH and Yang JH: starBase v2.0: Decoding miRNA-ceRNA, miRNA-ncRNA and protein-RNA interaction networks from large-scale CLIP-Seq data. Nucleic Acids Res 42: D92-D97, 2014.
28. Livak KJ and Schmittgen TD: Analysis of relative gene expression data using real-time quantitative PCR and the 2(-Delta Delta C(T)) method. Methods 25: 402-408, 2001.
29. Patop IL, Wüst S and Kadener S: Past, present, and future of circRNAs. EMBO J 38: e100836, 2019.
30. Fu Y, Dominissini D, Rechavi G and He C: Gene expression regulation mediated through reversible m□A RNA methylation. Nat Rev Genet 15: 293-306, 2014.
31. Einstein JM, Perelis M, Chaim IA, Meena JK, Nussbacher JK, Tankka AT, Yee BA, Li H, Madrigal AA, Neill NJ, *et al*: Inhibition of YTHDF2 triggers proteotoxic cell death in MYC-driven breast cancer. Mol Cell 81: 3048-3064, 2021.
32. Shi Y, Fan S, Wu M, Zuo Z, Li X, Jiang L, Shen Q, Xu P, Zeng L, Zhou Y, *et al*: YTHDF1 links hypoxia adaptation and non-small cell lung cancer progression. Nat Commun 10: 4892, 2019.
33. van Kouwenhove M, Kedde M and Agami R: MicroRNA regulation by RNA-binding proteins and its implications for cancer. Nat Rev Cancer 11: 644-656, 2011.
34. Mancarella C and Scotlandi K: IGF2BP3 from physiology to cancer: Novel discoveries, unsolved issues, and future perspectives. Front Cell Dev Biol 7: 363, 2019.
35. Lin CAOY, Chen ST, Jeng YM, Yeh CC, Chou HY, Deng YT, Chang CC and Kuo MYP: Insulin-like growth factor II mRNA-binding protein 3 expression promotes tumor formation and invasion and predicts poor prognosis in oral squamous cell carcinoma. J Oral Pathol Med 40: 699-705, 2011.
36. Chen P, Xu J, Cui Z, Wu S, Xie T and Zhang X: Multi-omics analysis of N6-methyladenosine reader IGF2BP3 as a promising biomarker in pan-cancer. Front Immunol 14: 1071675, 2023.
37. Han J and Hu X: IGF2BP3-stabilized SIX4 promotes the proliferation, migration, invasion and tube formation of ovarian cancer cells. Mol Med Rep 26: 232, 2022.
38. Zhu K, Gao T, Wang Z, Zhang L, Tan K and Lv Z: RNA N6-methyladenosine reader IGF2BP3 interacts with MYCN and facilitates neuroblastoma cell proliferation. Cell Death Discov 9: 151, 2023.
39. Lv L, Wei Q, Zhang J, Dong Y, Shan Z, Chang N, Zhao Y, Bian P and Yi Q: IGF2BP3 prevent HMGB1 mRNA decay in bladder cancer and development. Cell Mol Biol Lett 29: 39, 2024.
40. Zhang ZH, Wang Y, Zhang Y, Zheng SF, Feng T, Tian X, Abudurexiti M, Wang ZD, Zhu WK, Su JQ, *et al*: The function and mechanisms of action of circular RNAs in Urologic Cancer. Mol Cancer 22: 61, 2023.
41. Gu Z, Wu W, Lu J and Shen J: Construction of circular RNA-based competing endogenous RNA network in colon cancer. Precis Med Sci 13: 52-62, 2024.
42. Yang F, Ma Q, Huang B, Wang X, Pan X, Yu T, Ran L, Jiang S, Li H, Chen Y, *et al*: CircNFATC3 promotes the proliferation of gastric cancer through binding to IGF2BP3 and restricting its ubiquitination to enhance CCND1 mRNA stability. J Transl Med 21: 402, 2023.
43. Li Z, Ma G and Pan Y: Five circRNAs serve as potential diagnostic and prognostic biomarkers in lung adenocarcinoma. Clin Lab 67: 10-7754, 2021.
44. Mo Q, Qiu Y, Liang Y, Wei Q, Fan X and Pang W: Exploring long Noncoding RNAs and ferroptosis in cancer progression. Life Conflux 1: e128, 2025.

Copyright © 2026 Lai et al. This work is licensed under a Creative Commons Attribution-NonCommercial-NoDerivatives 4.0 International (CC BY-NC-ND 4.0) License.